Eur Biophys J (2001) 30: 75–81
DOI 10.1007/s002490000112

BIOPHYSICS LETTER

Matteo Dal Peraro · Frank Alber · Paolo Carloni

Ser133 phosphate-KIX interactions in the CREB-CBP complex: an ab initio molecular dynamics study

Received: 21 June 2000 / Revised version: 5 September 2000 / Accepted: 11 September 2000 / Published online: 30 November 2000

Abstract Cyclic AMP response element binding protein (CREB) is involved in activation of transcriptional DNA machinery by binding to the coactivator CREB-binding protein (CBP). The interactions between CREB serine phosphate (pSer133) and specific CBP residues (Tyr658 and Lys662) play a crucial role for the thermodynamic stability of the CREB-CBP complex. Here we use ab initio methods to investigate the dynamics and energetics of a relatively large, fully hydrated model complex representing pSer133 and its counterparts of the CBP domain. The calculations suggest that: (1) key contributions to the stabilization of the complex arise not only from electrostatics (as previously proposed) but also from a previously unrecognized "low-barrier hydrogen bond" between pSer133 and Lys662; (2) hydration plays a crucial role for the stabilization of the phosphate charge; (3) formation of the complex involves a significant degree of reorganization of the electronic charge density.

Key words Cyclic AMP response element binding protein · Phosphorylation · Car-Parrinello method · Density functional theory · Low barrier hydrogen bond

M. Dal Peraro · F. Alber · P. Carloni (✉)
International School for Advanced Studies,
SISSA, Via Beirut 4, 34014 Trieste, Italy
E-mail: carloni@sissa.it
Tel.: +39-040-3787407
Fax: +39-040-3787528

M. Dal Peraro
Dipartimento di Fisica "G. Galilei",
Università degli Studi di Padova, Padova, Italy

F. Alber · M. Dal Peraro · P. Carloni
Istituto Nazionale di Fisica della Materia, INFM, Italy

P. Carloni
International Centre for Genetic Engineering and Biotechnology,
ICGEB, Trieste, Italy

Introduction

Cyclic AMP (cAMP) response element binding protein (CREB) activates transcription of targeted genes (Hunter and Karin 1992). Activation is achieved by CREB kinase inducible domain (KID) binding to the KIX domain of the CREB-binding protein (CBP) (Chrivia et al. 1993; Kwok et al. 1994; Parker et al. 1996). An essential phosphorylated serine side chain belonging to KID (pSer133) promotes assembly of the KID-KIX complex by interacting with Tyr658 and Lys662 side chains of the KIX domain (Fig. 1a) (Radhakrishnan et al. 1997). pSer133 and Lys662 are partially inaccessible to the solvent whereas Tyr658 is completely buried inside the protein.

An elegant recent NMR investigation has shown that the contribution of phosphorylation to the overall stability of the complex is as large as −1.5(2) kcal/mol (Mestas and Lumb 1999). This is striking, as electrostatic interactions usually provide little net favorable contribution to subunit-subunit binding free energies (Hendsch and Tidor 1994; Lumb and Kim 1995). Indeed, the energy of the salt bridge, presumably very high, must be balanced against the partial or total hydration energy (which is also very high) of the groups involved. Furthermore, formation of salt bridges is unfavorable entropically. It has been postulated (Radhakrishnan et al. 1997; Mestas and Lumb 1999) that the unusual stabilization of the complex could arise from a combination of effects, including the reduced desolvation penalty of the KIX side chains upon binding to KID and the large phosphate-KIX electrostatic interactions in a low-dielectric medium.

To investigate the nature of the intriguing interactions between pSer133 and KIX, we have carried out quantum chemical calculations on a relatively large model (105 atoms). This complex contains all the groups interacting with pSer133 and it is fully hydrated (Fig. 1b). Our tool is the Car-Parrinello ab initio molecular dynamics (MD) method (Car and Parrinello

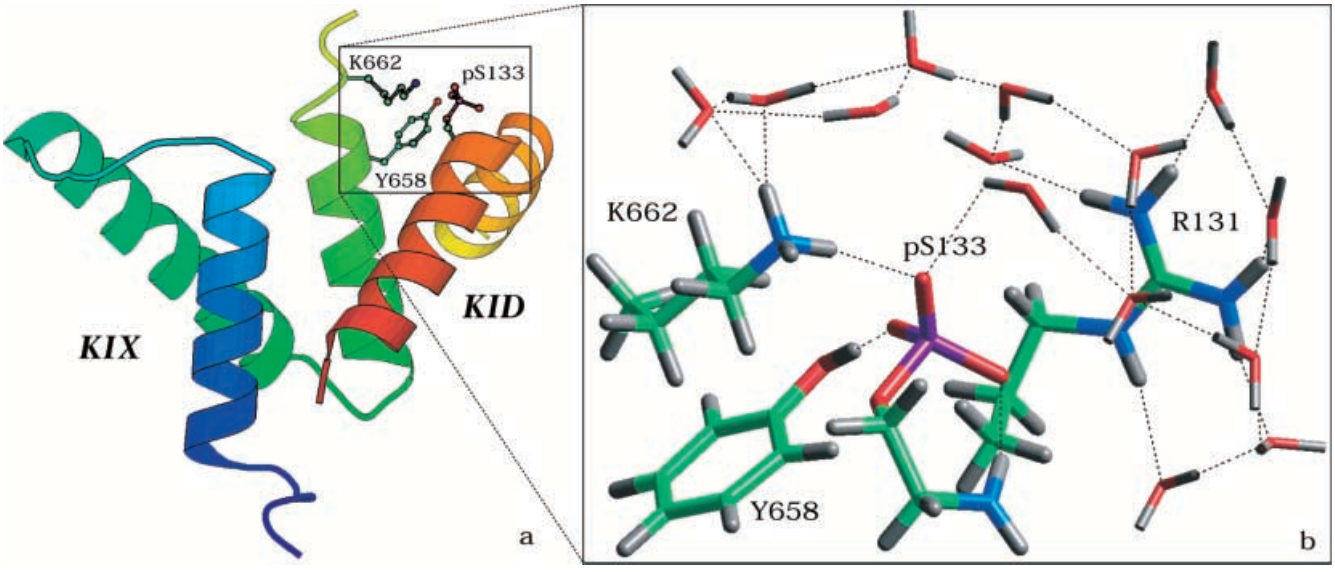

Fig. 1 **a** KID-KIX complex [entry 1kdx of PDB (Bernstein et al. 1999)]. pSer133, Tyr658, and Lys662 side chains are displayed in a *ball-and-stick model* [figure made with the MOLSCRIPT program (Kraulis 1997)]. **b** Fully hydrated quantum-mechanical model used in the calculations; *dashed lines* represent hydrogen bonds

1985). The approach appears to be favorable to investigate this problem in several respects. Based on density functional theory with gradient corrections, it allows a rather accurate description of relatively large systems at the ab initio level. Furthermore, it fully incorporates temperature effects, which are crucial for biological systems (Karplus and Petsko 1990). Finally, it has already been shown to reproduce accurately the structural and dynamical properties of phosphate esters moieties (Alber et al. 1999; Alber and Carloni 2000).

Materials and methods

Structural model

The structure of the KID-KIX complex in aqueous solution has been solved by NMR spectroscopy (Radhakrishnan et al. 1997). A family of 17 structures has been deposited in the Protein Data Bank (PDB) (Bernstein et al. 1999). We chose conformer 12, as in this structure pSer133 interacts both with Tyr658 [whose essential role for KIX-KID molecular recognition has been recently deciphered by site-directed mutagenesis experiments (Radhakrishnan et al. 1997)] and Lys662 [whose electrostatic interactions with pSer133 have been postulated to be crucial for KIX-KID binding (Mestas and Lumb 1999)]. Arg131 was also included to ensure electroneutrality in the system, although it belongs to the KID domain and does not participate in KIX-KID binding. pSer133, Tyr658, Lys662, and Arg131 side chains were modeled as 2-amino-1-phosphatoethane, phenol, 1-butylamine, and 1-propylguanidinium cation, respectively.

The final system also included 14 water molecules, equilibrated by classical molecular dynamics simulations and H-bonding to the complex (Fig. 1b). The initial positions of the water molecules (Fig. 1b) were obtained as follows. The complex was immersed in an orthorhombic box of $17.9 \times 13.3 \times 14.3$ Å^3 edges containing 92 water molecules. Then 100 ps of classical MD were carried out using the Dreiding 2.1 force field (Mayo et al. 1990). This simulation was performed in the canonical ensemble by coupling the system to a Nosé-Hoover thermostat (Nosé 1984; Hoover 1985) at a frequency of 500 cm^{-1}. Periodic boundary conditions were used, the electrostatic interactions being calculated with the Ewald summation method (Darden and York 1993). At the end of the simulation, all the molecules H-bonding to any group of the complex were included in the quantum-chemical model. The resulting number of water molecules was 14. During the dynamics the heavy atoms of the complex were kept fixed.

Quantum chemical calculations

Ab initio density functional theory calculations were carried out with two generalized gradient approximaton (GGA) exchange-correlation functionals. The first is the BLYP functional (Becke 1988; Lee et al. 1988), which has been shown to provide a reliable description of structural and dynamical properties of a variety of H-bonded systems (Sprik 1996; Alber et al. 1999; Carloni et al. 2000). However, it is known to underestimate energy barriers towards proton transfer (Sirois et al. 1997). The second is the new HCTH GGA functional (Hamprecht et al. 1998). Although HCTH has been tested in H-bonded systems to a lesser extent than BLYP, it has been shown to provide reliable reaction barriers in a variety of reactions and it is here used for comparison with the BLYP results.

The valence shell electrons are described by a plane wave basis set up to an energy cutoff of 70 Ry. The interaction between valence shell and core electrons is described by norm-conserving pseudopotentials of the Troullier-Martins type (Troullier and Martins 1991). The r_c values are reported below[1]. The complex was inserted in an orthorhombic supercell of $18.9 \times 16.0 \times 14.3$ Å^3 and was treated as an isolated system, following the method of Barnett and Landman (1993).

Ab initio density functional theory-based MD calculations (Car and Parrinello 1985) were performed in the canonical ensemble by coupling the system with a Nosé-Hoover (Nosé 1984; Hoover 1985) thermostat at a frequency of 500 cm^{-1} (Piana and Carloni 2000). A timestep of 0.121 fs and a fictitious electron mass of 1000 a.u. were used. We have imposed rigid position constraints on the terminal heavy atoms (Fig. 1b) in order to mimic the presence of the relatively rigid protein frame (De Santis and Carloni 1999; Piana and Carloni 2000).

[1]BLYP GGA TM pseudopotential r_c (expressed in Å): r_c(O) = 1.27 (s), 1.27 (p); r_c(C) = 1.23 (s), 1.23 (p); r_c(N) = 1.12 (s), 1.12 (p); r_c(P) = 1.45 (s), 1.60 (p), 1.60 (d). HCTH GGA TM pseudopotential r_c (expressed in Å): r_c(O) = 1.27 (s), 1.27 (p); r_c(C) = 1.23 (s), 1.23 (p); r_c(N) = 1.12 (s), 1.12 (p); r_c(P) = 1.40 (s), 1.40 (p), 1.40 (d).

Ab initio MD simulation with the BLYP GGA exchange-correlation functional was carried out for 1.0 ps at 150 K and 2.6 ps at 300 K. The last 2.5 ps were collected for analysis. The ab initio MD simulation with the HCTH functional was carried out for 0.05 ps at 150 K and 0.5 ps at 300 K.

We used a version of the Car-Parrinello code developed by Hutter et al. (1996), running on an SGI Origin 2000 parallel machine. One ab initio MD step required about 60 s of CPU time on 32 nodes.

Calculated properties

Electronic properties

Polarization effects are estimated by calculating the electronic density rearrangement upon complex formation: $\Delta\rho = \rho_{tot} - \rho_{pSer133} - \rho_{Lys662} - \rho_{Tyr658} - \rho_{water}$. The electronic structure is analyzed in terms of (1) Kohn-Sham orbitals; (2) electronic localization function (ELF) (Becke and Edgecombe 1990; Silvi and Savin 1994); and (3) the spread of the maximally localized Wannier orbitals (Marzari and Vanderbilt 1997; Silvestrelli et al. 1998).

Electrostatic interactions

Tyr658- and water-pSer133 electrostatic potential energies were calculated with the central multipolar expansion up to the second term. As the charge-charge terms are zero, E reads:

$$E(q,\mu) = \frac{q\mu\cos\theta}{4\pi\varepsilon_0 R^2} \quad (1)$$

where R is the absolute value of the distance vector (R) between the centers of charges of pSer133 and Tyr658 or the water molecules, q is the net charge of phosphate group, μ is the absolute value of the dipole moment (μ) of Tyr658 or the water molecules, and θ is the corresponding angle between R and μ vectors. The multipolar expansion is rigorously valid only for large R (Leach 1996). Its use here is limited to a qualitative comparison of energetics.

Structural properties

Coordination numbers (n_c) of phosphate oxygens are calculated as an integral of the radial distribution function (RDF) up to the first minimum (Sprik 1996).

Results

In this section we present results obtained with the BLYP (Becke 1988; Lee et al. 1988) gradient correction. Comparison is also made with results with the HCTH functional.

During the ab initio molecular dynamics, the Tyr658- and Lys662-pSer133 H-bonds are well maintained. Table 1 compares selected MD-averaged distances with respect to the NMR data. Notably, proton hopping between pSer133 and Lys662 H-bond donors occurs already in the picosecond timescale (Fig. 2a). This type

Table 1 Comparison between MD-averaged intermolecular distances (Å) and NMR data (Radhakrishnan et al. 1997). Labels as in Fig. 4

	Ab initio MD[a]	NMR
N(Lys662)-O1(pSer133)	2.9(3)	2.9
N(Lys662)-P(pSer133)	4.0(4)	3.8
H(Tyr658)-O2(pSer133)	1.8(1)	1.7
H(Tyr658)-P(pSer133)	3.1(1)	3.1
C(Arg131)-P(pSer133)	6.4(6)	5.8

[a] The MD averages refer to the simulation with the BLYP gradient correction

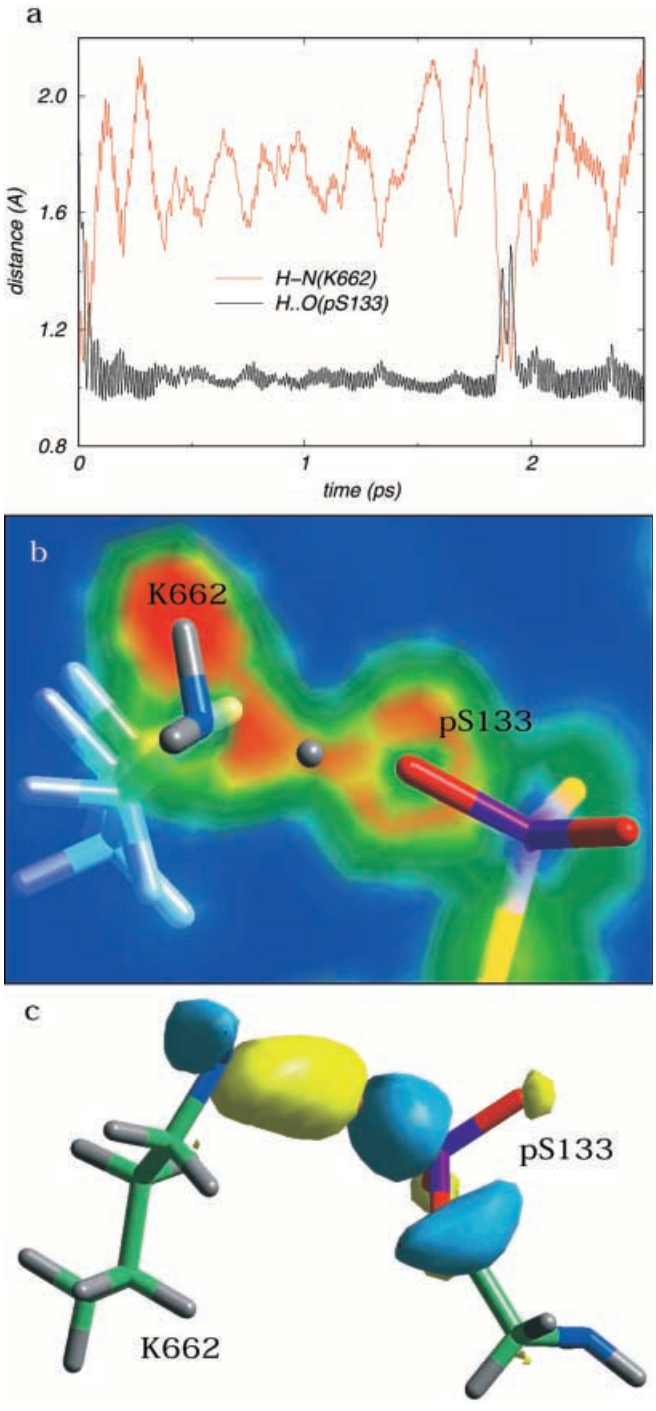

Fig. 2a–c pSer133-Lys662 salt bridge dynamics and electronic structure from BLYP GGA calculations (Becke 1988; Lee et al. 1988). **a** Plot of H-N(Lys662) and H-O(pSer133) distances versus time. **b** Electron localization function plotted on a plane containing the pSer133 oxygen, the proton, and Lys662 nitrogen during proton transfer. **c** Kohn-Sham molecular orbital for the same snapshot; in *yellow* (*light blue*) is represented positively (negatively) isodensity surface (10 a.u.)

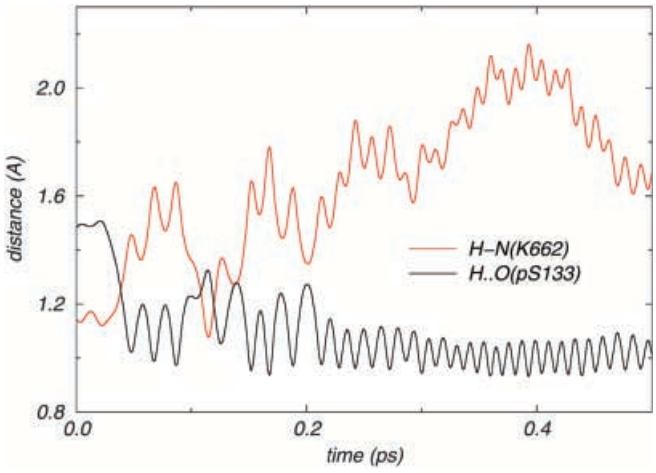

Fig. 3 pSer133-Lys662 salt bridge: results from the HCTH GGA calculations (Hamprecht et al. 1998). Plot of H-N(Lys662) and H-O(pSer133) distances versus time

of interaction is usually referred to as a "low-barrier hydrogen bond" (LBHB) (Cleland and Kreevoy 1994). As BLYP is known to underestimate proton transfer barriers (Sirois et al. 1997), we have carried out test calculations using the recently developed HCTH functional (Hamprecht et al. 1998), which provides a good description of hydrogen abstraction barriers. Figure 3 shows that the proton hopping occurs also with this gradient correction functional in the simulated time investigated (~0.5 ps).

To investigate the chemical bonding involved in the LBHB we calculate the electron localization function (ELF) during the proton transfer (Becke and Edgecombe 1990; Silvi and Savin 1994). The ELF efficiently illustrates chemical concepts such as localized bonds and electron lone pairs. Figure 2b indicates a high degree of electron localization between N(Lys662) and phosphate oxygen O(pSer133), suggesting that the interaction is partly covalent (De Santis and Carloni 1999).

Analysis of the bonding in terms of Kohn-Sham molecular orbitals on the same snapshot indicates that a covalent, three-center molecular orbital is formed (Fig. 2c). Consistent results are obtained by a calculation of the spread of maximally localized Wannier functions (Marzari and Vanderbilt 1997; Silvestrelli et al. 1998; Silvestrelli and Parrinello 1999). The calculated spreads increase from ~0.7 to ~0.8 a.u. during the proton transfer, confirming the delocalized nature of the bond. The covalency of the interaction, already postulated in different contexts (Gilli et al. 1994; Schiott et al. 1998), imposes a high level of directionality to the interaction, which could be important for the molecular recognition process.

The conformation of the phosphate moiety in pSer133 compares well with previous ab initio calculations and experimental data on the chemically similar dimethyl phosphate (Schneider et al. 1996; Alber et al. 1999). Table 2 shows that selected calculated structural parameters are in good accord with the two sets of data, except (as expected) for P-O1, which is involved in the proton hopping with Lys662.

pSer133 is highly hydrated. Integration of the O(pSer133)-O(water) RDF provides the coordination number (n_c). It turns out that, on average, 4.5 water molecules H-bond to phosphate during the dynamics.

pSer133-water interactions involve not only H-bonding but also electrostatics: water dipoles are partially aligned towards the phosphate oxygen atoms during the entire dynamics simulation (Fig. 4). Table 3 reports the energetics of the water molecules, which H-bond to phosphate for the entire simulation.

The double negative charge of pSer133 is further stabilized by H-bonding and electrostatic interactions with Tyr658. Figure 4 shows the optimal alignment of the Tyr658 electric dipole towards the phosphate charge, which is well maintained during the dynamics. However, Table 3 indicates that the order of magnitude of Tyr658-pSer133 interactions is much smaller than that of phosphate hydration.

All these interactions involve substantial polarization effects, as evidenced by the rearrangement of the electronic structure upon complex formation (Fig. 5).

Table 2 Comparison between selected MD-averaged structural parameters, previous ab initio DFT calculations with the same computational setup (Alber et al. 1999), and experimental values obtained by a statistical analysis of crystal structures of the chemically similar dimethyl phosphate (Schneider et al. 1996). Labels as in Fig. 4

	Ab initio MD[a]	(Alber et al. 1999)	(Schneider et al. 1996)
Bond distances (Å)			
P-O1	1.62(3)	1.49	1.51
P-O2	1.52(2)		
P-O3	1.52(2)		
P-O	1.66(4)	1.68	1.62
C-O	1.47(4)	1.44	1.43
Bond angles (deg)			
O-P-O1	104(3)	105	107
O-P-O2	105(4)	105	107
O-P-O3	110(3)	105	107
O1-P-O2	111(3)	118	113
O2-P-O3	118(3)	118	113
O3-P-O1	107(4)	118	113
C-O-P	122(4)	119	119

[a] The MD averages refer to the simulation with the BLYP gradient correction

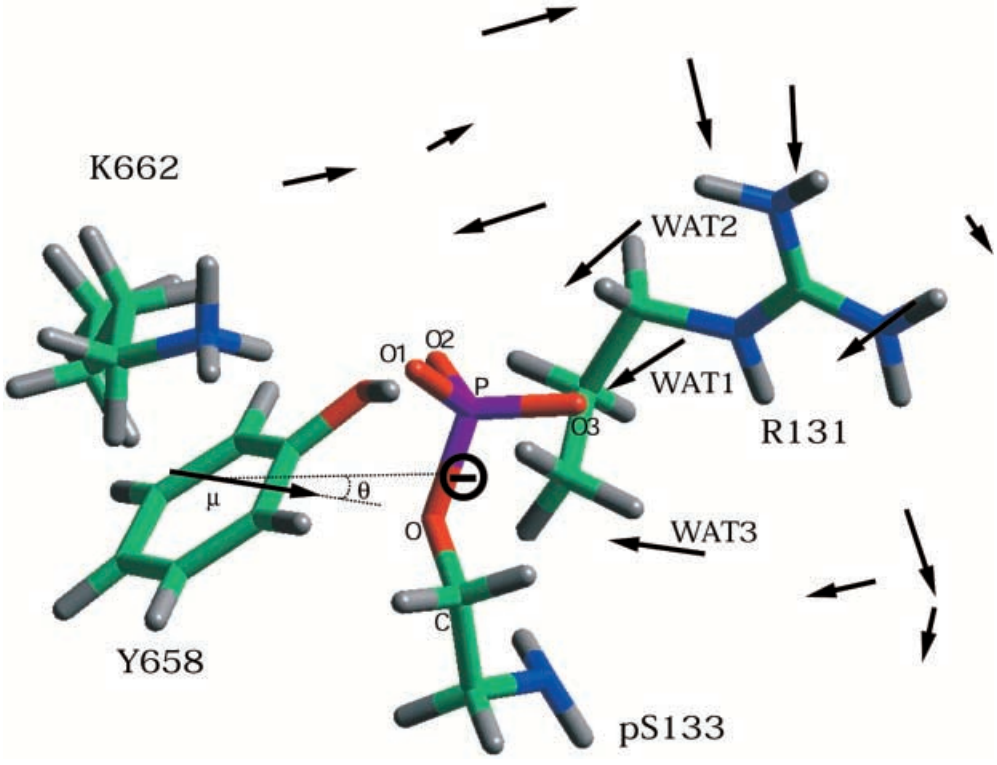

Fig. 4 Water and Tyr658 dipolar moments (μ) are superimposed on the molecular structure. The angle θ describes the relative orientation between the dipoles and the pSer133 center of charge

Table 3 Water- and Tyr658-pSer133 electrostatic interactions (E) derived by the charge-dipole term in the multipolar expansion. Values must be interpreted only for a qualitative comparison (see Materials and methods section). Only the energies of the three water molecules closest to phosphate (WAT1, WAT2, WAT3; see Fig. 4) are reported. θ and μ are defined in the Materials and methods section; Fig. 4 displays them for Tyr658

	E (kcal/mol)[a]	θ (deg)	μ (Debye)
WAT1	−11.0(5)	9(3)	2.2
WAT2	−8.0(6)	4(3)	2.1
WAT3	−4.8(5)	21(3)	2.1
Tyr658	−2.5(4)	32(5)	1.2

[a] The calculated values refer to the simulation with the BLYP gradient correction

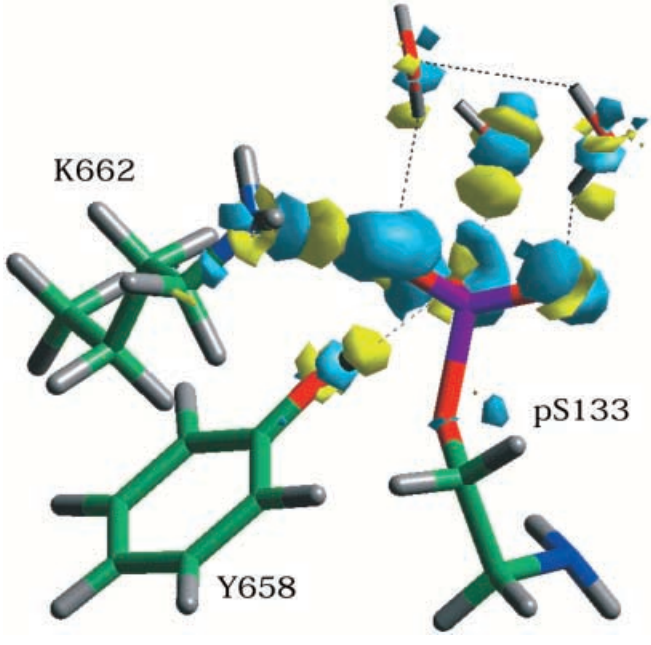

Fig. 5 Polarization effects: plot of electron density difference ($\Delta\rho = \rho_{tot} - \rho_{pSer133} - \rho_{Tyr658} - \rho_{Lys662} - \rho_{water}$) of the model complex. Positively (negatively) isodensity surfaces (0.005 a.u.) are drawn in *yellow* (*light blue*). Results obtained with the BLYP (Becke 1988; Lee et al. 1988) recipe for the exchange-correlation functional

Discussion

Our calculations suggest that a LBHB is formed between pSer133 and Lys662. This interaction turns out to be partly covalent in nature, as found in other contexts (Gilli et al. 1994; Schiott et al. 1998). This LBHB could be a key factor of the unexpectedly large stabilization of the pSer133-KIX complex. Indeed, this type of interaction is known to provide large stabilization energies (Cleland and Kreevoy 1994). Furthermore, the LBMB, by modifying the chemical environment and chemical properties of pSer133, could account for the decrease of the pSer133, pK_a by 1.1 units upon complex formation (Mestas and Lumb 1999).

A comment is due on the requirement of pK_a matching between H-bond donor and acceptor in LBHBs (Cleland and Kreevoy 1994). The pK_as of Lys and 1-amino-2-phosphatoethane (our model for pSer133) differ by more than 3 units, yet the difference in pK_a could be dramatically reduced in the presence of a

low-dielectric medium such in the KID-KIX interface (Mestas and Lumb 1999). Similar considerations have been invoked to explain a LBHB between Asp102 and His57 in the active site of serine protease and a specific H-bond pattern in the active site of Zn carboxypeptidase (Mangani et al. 1992; Frey et al. 1994).

In the LBHB, the proton hops already in the subpicosecond timescale. This high proton hopping frequency may be due to the limited size of the protein complex used here (Piana and Carloni 2000). We may expect that the use of larger models and/or of QM/MM approaches could affect the timescale of the process.

Our calculations allow also for identifying the nature of the interactions between pSer133 and the other surrounding groups. The phosphate negative charge is stabilized by charge-dipole and H-bonding interactions with Tyr658 (Fig. 4). Loss of these interactions with Y658F (and Y658A) KIX mutants provides the physical origin of the reduced (abrogated) complex affinity (Radhakrishnan et al. 1997).

Hydration stabilizes the phosphate even more. Figure 4 shows a high degree of alignment of water dipoles towards the phosphate oxygens, similar to what has been found in force-field molecular dynamics simulations of a phospholipid membrane bilayer (Tu et al. 1996). Thus, hydration emerges as a key factor for phosphate charge stabilization.

In conclusion, the ab initio quantum chemical calculations presented here suggest that a low-barrier H-bond – an interaction other than electrostatic – may play a crucial role for the striking stability of the pSer133-KIX complex. Thus, phosphorylation could use the large LBHB stabilization to help promote complex formation. Furthermore, hydration appears to play a crucial role for the stabilization of the phosphate charge. Finally, complex formation involves a substantial rearrangement of the electronic charge density (Fig. 5). Hence, analysis of the molecular interactions of the KID-KIX complex in terms of simple electrostatic models might therefore require an explicit description of polarization effects.

Acknowledgements We thank COFIN and INFM for support, EC-ICARUS project and CINECA for generous amounts of computer time. One of us (M.D.P.) thanks SISSA for financial support. Useful discussions with Antonino Cattaneo are also acknowledged.

References

Alber F, Carloni P (2000) Ab initio molecular dynamics studies on HIV-1 reverse transcriptase triphosphate binding site: implications for nucleoside-analog drug resistance. Protein Sci (in press)

Alber F, Folkers G, Carloni P (1999) Dimethyl phosphate: stereoelectronic versus environments effects. J Phys Chem B 103: 6121–6126

Barnett RN, Landman U (1993) Born-Oppeneimer molecular dynamics simulations of finite systems: structure and dynamics of $(H_2O)_2$. Phys Rev B 48: 2081–2097

Becke AD (1988) Density-functional exchange-energy approximation with correct asymptotic behavior. Phys Rev A 38: 3098–3100

Becke AD, Edgecombe KE (1990) A simple measure of electron localization in atomic and molecular systems. J Chem Phys 92: 5397–5403

Bernstein FCL, Koetzle TF, Williams GJB (1999) The protein data bank: a computer-based archival file for macromolecular structures. J Mol Biol 112: 535–542

Car R, Parrinello M (1985) Unified approach for molecular dynamics and density-functional theory. Phys Rev Lett 55: 2471–2474

Carloni P, Sprik M, Andreoni W (2000) Key steps of the cisplatin-DNA interaction: density functional theory-based molecular dynamics simulations. J Phys Chem 104: 823–835

Chrivia JC, Kwok RP, Lamb N, Hagiwara M, Montminy MR, Goodman RH (1993) Phosphorylated CREB binds specifically to the nuclear protein CBP. Nature 365: 855–859

Cleland WW, Kreevoy MM (1994) Low-barrier hydrogen bonds and enzymic catalysis. Science 264: 1887–1890

Darden, TA, York D (1993) Particle mesh Ewald: an N log(N) method for Ewald sums in large systems. J Chem Phys 98: 10089–10094

De Santis L, Carloni P (1999) Serine proteases: an ab initio molecular dynamics study. Proteins Struct Funct Genet 37: 611–618

Frey PA, Whitt SA, Tobin JB (1994) A low-barrier hydrogen bond in the catalytic triad of serine proteases. Science 264: 1927–1930

Gilli P, Bertolasi V, Ferretti V, Gilli G (1994) Covalent nature of the strong homonuclear hydrogen bond. Study of the O-H-O system by crystal structure correlation methods. J Am Chem Soc 116: 909–915

Hamprecht FA, Cohen AJ, Tozer DJ, Handy NC (1998) Development and assessment of new exchange-correlation functionals. J Chem Phys 109: 6264–6271

Hendsch ZS, Tidor B (1994) Do salt bridges stabilize proteins? A continuum electrostatic analysis. Protein Sci 3: 211–226

Hoover WG (1985) Canonical dynamics: equilibrium phase-space distribution. Phys Rev A 31: 1695–1697

Hunter T, Karin M (1992) The regulation of transcription by phosphorylation. Cell 70: 375–387

Hutter J, Ballone P, Bernasconi N, Focher P, Fois E, Godecker S, Parrinello M, Tuckerman M (1996) CPMD. MPI fur Festkorperforschung and IBM Research Laboratory, Zurich

Karplus M, Petsko GA (1990) Molecular dynamics simulations in biology. Nature 347: 631–639

Kraulis P (1997) MolScript v2.1. Avatar Software, Stockholm; www.avatar.se/molscript

Kwok RP, Lundblad JR, Chrivia JC, Richards JP, Bachinger HP, Brennan RG, Roberts SG, Green MR, Goodman RH (1994) Nuclear protein CBP is a coactivator for the transcription factor CREB. Nature 370: 223–226

Leach A (1996) Molecular modeling: principles and applications. Longman, Harlow, UK, pp 148–171

Lee C, Yang W, Parr RG (1988) Development of the Colle-Salvetti correlation-energy formula into a functional of the electron density. Phys Rev B 37: 785–789

Lumb KJ, Kim PS (1995) Measurement of interhelical electrostatic interactions in the GCN4 leucine zipper. Science 268: 436–439

Mangani S, Carloni P, Orioli P (1992) Crystal structure of the complex between carboxypeptidase A and the byproduct analog inhibitor L-benzylsuccinate at 2.0 Å resolution. J Mol Biol 223: 573–578

Marzari N, Vanderbilt D (1997) Maximally-localized Wannier functions for composite energy bands. Phys Rev B 56: 12847–12865

Mayo SL, Olafson BD, Goddard WA (1990) Dreiding: a generic force field for molecular simulations. J Phys Chem 94: 8897–8909

Mestas SP, Lumb KJ (1999) Electrostatic contribution of phosphorylation to the stability of the CREB-CBP activator-coactivator complex. Nat Struct Biol 6: 613–614

Nosé SJ (1984) A unified formulation of the constant temperature molecular dynamics methods. J Chem Phys 81: 511–519

Parker D, Ferreri K, Nakajima T, LaMorte VJ, Evans R, Koerber SC, Hoeger C, Montminy MR (1996) Phosphorylation of CREB at Ser-133 induces complex formation with CREB-binding protein via a direct mechanism. Mol Cell Biol 16: 694–703

Piana S, Carloni P (2000) Conformational flexibility of the catalytic asp dyad in HIV-1 protease: an ab initio study on the free enzyme. Proteins 39: 26–36

Radhakrishnan I, Perez-Alvarado GC, Parker D, Dyson HJ, Montminy MR, Wright PE (1997) Solution structure of the KIX domain of CBP bound to the transactivation domain of CREB: a model for activator:coactivator interactions. Cell 91: 741–752

Schiott B, Iversen BB, Madsen GK, Larsen FK, Bruice TC (1998) On the electronic nature of low-barrier hydrogen bonds in enzymatic reactions. Proc Natl Acad Sci USA 95: 12799–12802

Schneider B, Kabelac M, Hobza P (1996) Geometry of the phosphate group and its interactions with metal cations in crystals and ab initio calculations. J Am Chem Soc 118: 12207–12217

Silvestrelli PL, Parrinello M (1999) Water molecular dipole in the gas and in the liquid phase. Phys Rev Lett 82: 3308–3311

Silvestrelli PL, Marzari N, Vanderbilt D, Parrinello M (1998) Maximally-localized Wannier functions for disordered systems: application to amorphous silicon. Solid State Commun 107: 7–11

Silvi B, Savin A (1994) Classification of chemical bonds based on topological analysis of electron localization functions. Nature 371: 683–686

Sirois S, Proynov EI, Nguyen DT, Salahub DR (1997) Hydrogen-bonding in glycine and malonaldehyde: performance of the Lap1 correlation functional. J Chem Phys 107: 6770–6781

Sprik M (1996) Ab initio molecular dynamics simulation of liquids and solutions. J Phys Condens Matter 8: 9405–9409

Troullier N, Martins JL (1991) Efficient pseudopotentials for plane-wave calculation. Phys Rev B 43: 1943–2006

Tu K, Tobias DJ, Blasie JK, Klein ML (1996) Molecular dynamics investigation of the structure of a fully hydrated gel-phase dipalmitoylphosphatidylcholine bilayer. Biophys J 70: 595–608